Frequency encoding in renal blood flow regulation

Donald J. Marsh, Olga V. Sosnovtseva, Alexey N. Pavlov, Kay-Pong Yip and Niels-Henrik Holstein-Rathlou

Am J Physiol Regul Integr Comp Physiol 288:1160-1167, 2005. First published Jan 20, 2005;
doi:10.1152/ajpregu.00540.2004

Am J Physiol Regul Integr Comp Physiol 288: R1160–R1167, 2005.
First published January 20, 2005; doi:10.1152/ajpregu.00540.2004.

Frequency encoding in renal blood flow regulation

Donald J. Marsh,[1] Olga V. Sosnovtseva,[2] Alexey N. Pavlov,[3] Kay-Pong Yip,[4] and Niels-Henrik Holstein-Rathlou[5]

[1]*Department of Molecular Pharmacology, Physiology, and Biotechnology, Brown University, Providence, Rhode Island;* [2]*Department of Physics, Danish Technical University, Lyngby, Denmark;* [3]*Department of Physics, Saratov State University, Saratov, Russia;* [4]*Department of Physiology & Biophysics, University of South Florida, Tampa, Florida; and* [5]*Department of Medical Physiology, Panum Institut, University of Copenhagen, Copenhagen N, Denmark*

Submitted 9 August 2004; accepted in final form 19 January 2005

Sosnovtseva, Donald J. Marsh, Olga V., Alexey N. Pavlov, Kay-Pong Yip, and Niels-Henrik Holstein-Rathlou. Frequency encoding in renal blood flow regulation. *Am J Physiol Regul Integr Comp Physiol* 288: R1160–R1167, 2005. First published January 20, 2005; doi:10.1152/ajpregu.00540.2004.—With a model of renal blood flow regulation, we examined consequences of tubuloglomerular feedback (TGF) coupling to the myogenic mechanism via voltage-gated Ca channels. The model reproduces the characteristic oscillations of the two mechanisms and predicts frequency and amplitude modulation of the myogenic oscillation by TGF. Analysis by wavelet transforms of single-nephron blood flow confirms that both amplitude and frequency of the myogenic oscillation are modulated by TGF. We developed a double-wavelet transform technique to estimate modulation frequency. Median value of the ratio of modulation frequency to TGF frequency in measurements from 10 rats was 0.95 for amplitude modulation and 0.97 for frequency modulation, a result consistent with TGF as the modulating signal. The simulation predicted that the modulation was regular, while the experimental data showed much greater variability from one TGF cycle to the next. We used a blood pressure signal recorded by telemetry from a conscious rat as the input to the model. Blood pressure fluctuations induced variability in the modulation records similar to those found in the nephron blood flow results. Frequency and amplitude modulation can provide robust communication between TGF and the myogenic mechanism.

tubuloglomerular feedback; myogenic mechanism; nonlinear interactions; amplitude modulation

TUBULOGLOMERULAR FEEDBACK (TGF) and the myogenic mechanism regulate renal blood flow and glomerular filtration rate (GFR) of individual nephrons. Each generates an oscillation (7, 9, 14–17, 25) that originates in nonlinearities of the particular system, and each acts on afferent arterioles. Because an afferent arteriolar smooth muscle cell has only one contractile mechanism, the two controllers must interact within single muscle cells. We have developed a computer simulation that models the interaction and predicts renal plasma flow, GFR, tubular hydrostatic pressure, NaCl concentration in tubular fluid at the macula densa, as well as a number of intracellular variables in arteriolar smooth muscle. The model permits comparison with experimental measurements of the plasma flow (25), the tubular variables, and GFR (7, 9, 14–17). The model is the combination of a model of tubular pressure and flow and tubular NaCl concentration in a compliant tubule with reabsorption of solute and water (6, 8), a model of glomerular filtration (4), and a model of cerebral arteriolar vasomotion (5), modified for use in the kidney. The model presented in this and an accompanying paper (18) couples TGF to voltage-gated Ca channels, and a comparison of the model predictions with experimental results provides a test of the coupling site.

Simulation results with the model predicted that TGF modulates both the amplitude and the frequency of the myogenic oscillation, a result that has not been reported in the experimental literature. Frequency modulation is a variation in time of the frequency of an oscillation, and the two forms of modulation can arise because of nonlinear interactions with another oscillator. Standard spectral techniques assume that the signal being measured is stationary, a condition violated when there is frequency or amplitude modulation. We turned to wavelet transforms to measure the two forms of modulation (3). Wavelets are mathematical functions that represent a class of single waves that are soliton-like. The process of convolving them with time series, known as wavelet transforms, can provide separate measures of amplitude and frequency as continuous functions of time. We applied wavelet transforms to previously published results of blood flow in single renal efferent arterioles (25) and to the simulation results. The analysis confirmed the presence of amplitude and frequency modulation in the experimental results; the modulating frequency was the same as the frequency of the TGF oscillation. The results of these analyses are also presented in this paper. The comparison of simulation and experimental results is consistent with coupling of TGF to voltage-gated Ca channels.

The modulation measured from experimental results is more variable than the simulation predicts. We used arterial blood pressure records obtained by telemetry from normotensive rats as an input to the model. The result indicates that fluctuations of arterial pressure contribute to the variability of frequency and amplitude modulation.

METHODS

Experimental methods. The experimental data were from two previous studies (10, 25). In measurements of single-nephron efferent arteriolar blood flow, normal Sprague-Dawley rats were anesthetized with a gas mixture of halothane, nitrogen, and oxygen. The left kidney was exposed. The beam of a He-Ne laser was passed through an optical fiber to a GRIN-rod lens to reduce the beam diameter, and it was aimed at a single efferent arteriole on the surface of the kidney. The scattered light was collected with a second fiber, and Doppler frequency shifts were measured to determine relative velocity changes in blood flow. Details of the method are found in Ref. 23.

In the second study, Sprague-Dawley and spontaneously hypertensive rats rats were anesthetized with pentobarbital to permit the

Address for reprint requests and other correspondence: Donald J. Marsh, Dept. Mol. Pharmacol. Physiol. & Biotechnol., Brown Univ., Box G-B593, Providence, RI 02912 (E-mail: marsh@ash.biomed.brown.edu).

The costs of publication of this article were defrayed in part by the payment of page charges. The article must therefore be hereby marked "*advertisement*" in accordance with 18 U.S.C. Section 1734 solely to indicate this fact.

implantation of a blood pressure transducer, radio transmitter, and battery. A needle filled with a proprietary anticoagulant gel was inserted into the abdominal aorta, and the rest of the device was placed in the abdominal cavity. The incision was closed, and the rat was allowed to recover. After a suitable postoperative period, the rat was placed in a cage with a radio receiver nearby, and the blood pressure was recorded while the rat was free to move about the cage. Food and water were provided to the rat on the same schedule as to all other rats in the colony. The signal was passed through an analog low-pass filter with a cutoff frequency of 3 Hz, which was sufficient to remove the fluctuation due to the heart rate. Details are found in Ref. 10. Only results from normotensive rats are used in this paper.

Wavelet transforms. Preliminary model results with membrane-based coupling sites gave evidence of amplitude and frequency modulation of the faster oscillation by the slower one. Frequency modulation is an example of nonlinear interaction; amplitude modulation can arise from either a linear or nonlinear interaction. The equations we derived to model the interaction are nonlinear (18). Frequency and amplitude modulation can easily be seen and measured in the model results run at constant arterial pressure, but not in model results run with variable arterial pressure (18), or in results of experimental studies (see below). A uniform method was therefore needed for the analysis of all results. Standard spectral methods can give some information on the modulation process, but they are unable to separate the two forms if they coexist. We therefore made use of wavelet analysis, a class of analytic techniques that are well designed for such problems. The method provides an opportunity to study the temporal evolution of signals with different rhythmic components.

The wavelet transform of a signal $x(t)$ is performed by convolving a wavelet function with the signal, as follows:

$$T_x(a,t) = \frac{1}{\sqrt{a}} \int_{-\infty}^{\infty} x(u)\psi^*\left(\frac{u-t}{a}\right)du \qquad (1)$$

where

$$\frac{1}{\sqrt{a}}\psi\left(\frac{u-t}{a}\right)$$

is a function constructed from a "mother" wavelet $\psi(u)$ using scaling and translation. The latter wavelet is a function that, in general, can have an arbitrary shape provided it is soliton-like; that is, is localized over a time interval and has a zero average in time. The $T_x(a,t)$ are the wavelet coefficients, a is a time scale parameter, t is time, and the asterisk refers to the complex conjugate. In the analysis of various rhythmic components the so-called Morlet function is often applied. Its simplified expression appropriate to the study of low-frequency dynamics has the following form:

$$\psi(\tau) = \pi^{1/4} \exp(j2\pi\tau) \exp\left[-\frac{\tau^2}{2}\right], \quad \tau = \frac{u-t}{a} \qquad (2)$$

The wavelet represents a harmonic oscillation with frequency $f = 1/a$ (angular frequency $2\pi f$) and with amplitude modified in time by a Gaussian factor that describes how the wave arises and decays. Hereafter, we consider the time–frequency representation of the wavelet transform. With this, the coefficients $T_x(f,t)$ measure the spectral contribution near the frequency f at time t of the observed signal. In addition to the wavelet transform coefficients $T_x(f,t)$, we estimated the energy density, $E_x(f,t)$, from

$$E_x(f,t) = f\,C\,|T_x(f,t)|^2 \qquad (3)$$

where $a = 1/f$ is a time scale and C is a constant chosen dependent on the form of ψ. The result is a surface in three-dimensional space $E_x(f,t)$, with well-defined ridges corresponding to different oscillatory modes in the signal. Sections of this surface at fixed moments of $t = t_0$ correspond to the local energy spectrum. At each sampled moment of time, the maxima of the local spectra provide frequencies and amplitudes of the rhythmic components. The instantaneous frequencies and amplitudes are then analyzed for entrainment and modulation of those various rhythmic components.

There is a complication with the application of wavelet methods that is specific to the renal blood flow data. All methods suppose that a spectrum is calculated within some data window. To obtain proper results, the spectral components, such as the frequencies being estimated, should be nearly constant within this window. In the case of wavelet analysis, this means that during 5–6 oscillations of the fast mode, the corresponding frequency should not change significantly. In our experience, this condition is usually satisfied if the modulated frequency is about 30 times the modulating frequency, but the ratio of the two oscillations for nephron data is 5:1. In the data we wish to analyze, there will be significant violation of any assumption of constant frequency within even the smallest useful sampling window. The limited resolution that would be imposed could produce spurious peaks in the modulation spectrum.

To solve the problem created by the relatively small ratio between the two frequencies, we estimated the modulation properties of the signal by introducing the following procedure:

1. From the original signal $x(t)$, extract the time dependencies of the instantaneous frequencies f_{fast} and f_{slow} related to the fast and slow oscillatory modes, respectively, using wavelet analysis. These frequencies are identified using the energy spectrum, equation (3), by taking the energy maxima in the frequency bands 0.02–0.05 Hz for $f_{slow}(t)$, and 0.1–0.2 Hz for $f_{fast}(t)$. The two frequencies are identified for each time point, t_i, and a new time series is constructed from the frequencies in the energy spectrum at each of the time points in the original time series.

2. $f_{fast}(t)$ is used now as the input signal for the next wavelet transform, that is, we take $f_{fast}(t)$ instead of $x(t)$ in *Eq.* (1). Again, the wavelet coefficients and the energy density are estimated. The latter will contain information about all modes involved in the modulation process. Instead of the instantaneous frequency of the fast dynamics, we can take the instantaneous amplitude of this oscillatory mode and, therefore, it is possible to study the properties of amplitude modulation of the fast rhythm as well. The frequency resolution of the method is ~0.01 Hz.

Model. The model and the numerical methods used to solve it are presented in detail in the accompanying paper (18). The model consists of three partial differential equations that describe pressure, flow, and NaCl concentration as functions of time and distance along the nephron, one initial valued ordinary differential equation that describes the rate of change of protein concentration in glomerular capillaries as a function of distance, and six initial valued ordinary differential equations that describe the rates of change of a number of intracellular variables in each of two afferent arteriolar segments. The input to the arteriolar models is the arterial pressure, and the model predicts the segmental resistance to flow, from which the GFR and renal plasma flow are calculated.

RESULTS

Simulation results. Fig. 1 shows the simulated nephron plasma flow rate and the power spectrum generated from it. The frequency of the TGF oscillation is 0.023 Hz, and there is spectral power distributed in several peaks from 0.07 to 0.16 Hz. Much of the spectral power in this frequency band is generated from nonlinear interactions, as described in the accompanying paper (18). Spectra published with the original report of the single-nephron efferent blood flow data were obtained with different methods than the fast Fourier transform (FFT) used here (25). Yip et al. used a low-pass Kaiser-Bessel filter and an autoregressive spectral technique. Both techniques are designed to remove noise, and the resulting spectrum had

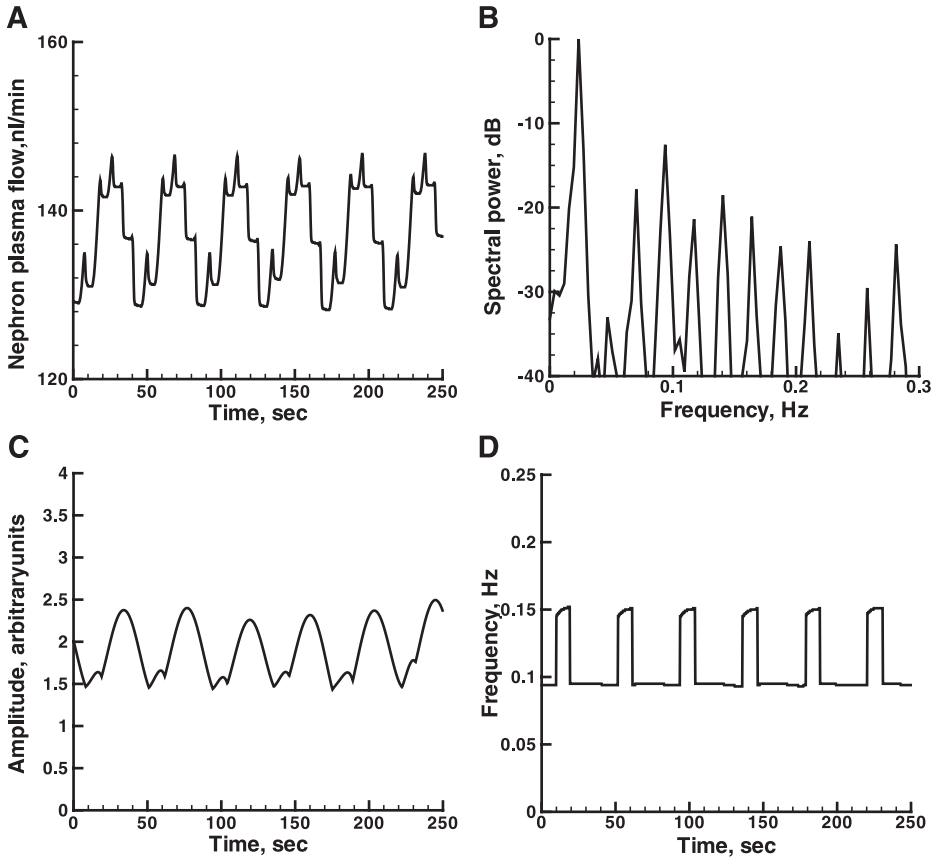

Fig. 1. Simulation results: TGF coupled to voltage-gated Ca channels. *A*: nephron plasma flow. [From Ref. 18.] The variable in (*A*) is nephron plasma flow, 0–200 nl/min. *B*: power spectrum of nephron plasma flow shown in left panel. [From Ref. 18.] *C*: instantaneous amplitude of the myogenic oscillation. *D*: instantaneous frequency of the myogenic oscillation.

fewer details in the 0.07 to 0.16 Hz band than does the spectrum in Fig. 1. Fig. 1 also shows the results of wavelet transforms applied to the simulated nephron plasma flow data. Both the instantaneous amplitude and frequency of the myogenic oscillation vary with time. As can be seen from the Fig. 1, both amplitude and frequency of the myogenic process fluctuate in synchrony with the TGF oscillation. The myogenic frequency in the model switches back and forth between 0.096 and 0.141 Hz. There are spectral peaks at these frequencies, and as argued in the accompanying paper, at least, part of the spectral power is generated by the primary oscillation of the myogenic mechanism, and the rest by nonlinear interactions (18). Analytic methods currently available do not permit a resolution of the contribution of these different sources of spectral power. The specific prediction of this simulation is that the TGF signal, conducted to voltage-gated Ca channels, leads to amplitude and frequency modulation of the myogenic oscillation.

Wavelet transforms of single-nephron blood flow measurements. Figure 2*A* shows the record of a measurement of efferent arteriolar blood flow in a rat taken from the results published in (25), Fig. 2*B* contains the mean arterial blood pressure recorded at the same time as the efferent arteriolar blood flow, and Fig. 2*C* shows the power spectrum of the efferent arteriolar flow record, calculated with an FFT. The slow oscillation typical of TGF can be seen in the record and is the largest peak of the power spectrum. The record also shows higher frequency fluctuations, corresponding to which the power spectrum shows peaks at frequencies higher than the large, slow oscillation. As shown in the accompanying paper, a collection of peaks like those in Fig. 2*B* can result from nonlinear interactions between TGF and the myogenic mechanism (18).

Figure 3, *A* and *B* presents the results of wavelet transforms applied to the record of Fig. 2. Fig. 3*A* shows the instantaneous amplitude of the high-frequency oscillation as a function of time and reflects amplitude modulation of the vasomotion. This result is the product of a nonlinear interaction. Figure 3*B* shows the instantaneous frequency of the fast oscillation as a function of time. Note that frequency is not constant but varies with time, also reflecting a nonlinear interaction.

Figures 4, *A* and *B* shows the instantaneous TGF frequency as a function of time, as well as the frequencies at which the curves in Fig. 3, *A* and *B*, respectively, are being modulated. The curves in Fig. 4, *A* and *B* were derived by applying the second-wavelet transform to the data of Fig. 3, *A* and *B*, as described in METHODS. During the course of the experiment, the frequency of the TGF oscillation varied between 0.028 and 0.034 Hz. The frequency of the amplitude modulation varied between 0.019 and 0.034 Hz, while the frequency of the frequency modulation varied between 0.020 and 0.031 Hz. In each case, the modulation frequency and the TGF frequency were operating in approximately the same bandwidth, an observation consistent with the suggestion that TGF operates to modulate both the amplitude and the frequency of the myogenic oscillation.

Because there was some variation in both the TGF frequency and the modulation frequency during the course of individual experiments, we used the wavelet transform to calculate the instantaneous frequency of each of the two curves represented

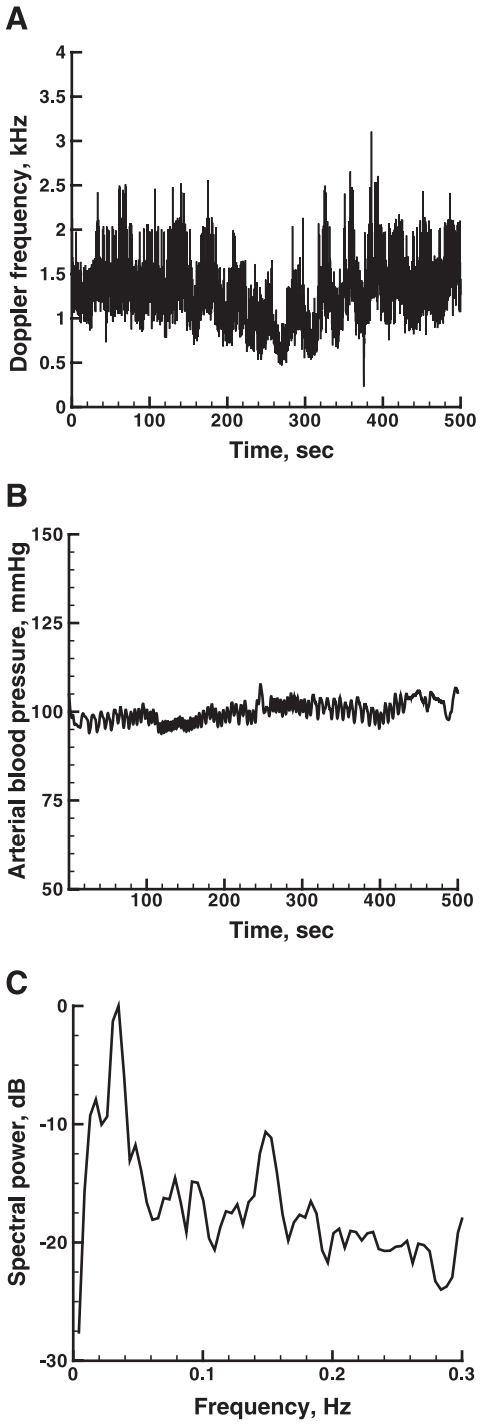

Fig. 2. *A*: recording of relative changes in single-nephron blood flow from one efferent arteriole. [From Ref. 25.] The variable in Fig. 2 is the laser-Doppler frequency shift, 0–5 kHz. *B*: recording of arterial blood pressure during the recording in (*A*). *C*: power spectrum from the record in (*A*).

in Fig. 4, *A* and *B*. Ten experiments, each sampled at 8.9 Hz, provided a total of around 50,000 individual data points, allowing the same number of calculations of instantaneous frequency. We divided the instantaneous frequency of the amplitude modulation curve by the instantaneous frequency of the slow oscillation. The results are in Fig. 5*A*. A similar calculation was done for frequency modulation, and the results are in Fig. 5*B*. For both the amplitude and the frequency measures, the ratio of modulation to TGF frequency clustered around unity. The median value of this ratio was 0.95 for amplitude modulation, and 0.97 for frequency modulation. The estimated modulation frequency is close to the TGF frequency but can be shifted to either side. Deviations of about 0.01 Hz can be attributed to the resolution of the method for estimation of instantaneous frequencies. The results of Fig. 5, *A* and *B* are also consistent with amplitude and frequency modulation of the myogenic oscillation by TGF.

From these analyses, we conclude that experimental results show both amplitude and frequency modulation of myogenic vasomotion by TGF.

Blood pressure fluctuations and frequency modulation. The simulation results of Fig. 1 show nearly perfect regularity in the amplitude and frequency modulation, whereas the experimental results in Fig. 3 show considerable variability in these measures. One possible difference in the conditions between the two is that the simulation was conducted with constant blood pressure, while the experiments were done with the fluctuations in arterial blood pressure that are normally present (10). Therefore, we used blood pressure records made by telemetry from conscious Sprague-Dawley rats to determine

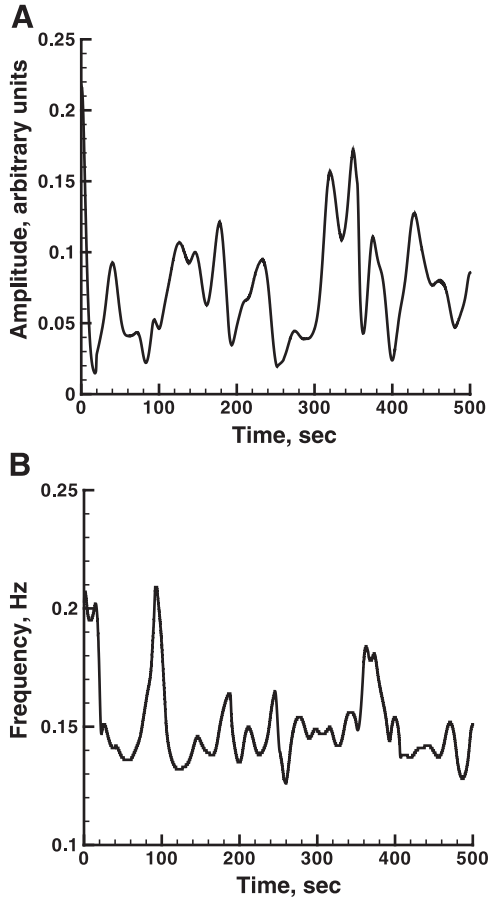

Fig. 3. Results of wavelet transforms applied to the nephron blood flow data in Fig.2. *A*: amplitude modulation. *B*: frequency modulation. Arbitrary units for amplitude modulation are derived from the scale of the variable, which in this figure is the laser-Doppler frequency shift, 0–5 kHz. The variable in Fig. 1*A* is nephron plasma flow, 0–200 nl/min. The arbitrary units are therefore not the same as in Fig. 1.

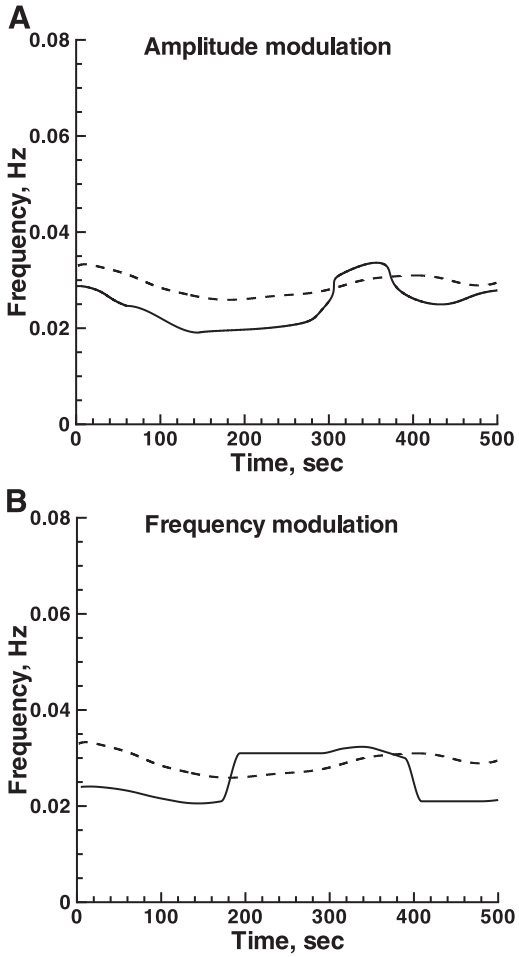

Fig. 4. The frequencies at which the amplitude (*A*) and the frequency (*B*) of single-nephron blood flow of Fig. 2 are modulated (solid lines) and the frequency of TGF (dashed line). The dashed lines are the same in the two panels.

whether the blood pressure fluctuations might be responsible for the changing modulation. Fig. 6 contains the results. The arterial pressure record shown in Fig. 6*A* was used as an input to the same model as was used in the simulation of Fig. 1. The predicted nephron plasma flow rate shows prominent oscillations at the TGF frequency and higher-frequency smaller-amplitude oscillations as well. The amplitude of the TGF oscillations varies with the arterial pressure, higher pressures generating larger oscillations. Because TGF is coupled to voltage-gated Ca channels, the variation in the amplitude of TGF oscillations sets the stage for variation in the amplitude and frequency of the myogenic oscillation. Figure 6, *C* and *D* show the instantaneous amplitude and frequency calculated by wavelet transforms from the predicted nephron plasma flow rate. As can be seen, the amplitude and frequency vary in an irregular pattern, as is the case in the experiment shown in Fig. 3. The range of the amplitude modulation in Figs. 3 and 6 cannot be compared directly because, as explained in the legend to Fig. 3, the units are different. The frequency modulation in Fig. 6 varies over a greater range of frequencies than in Fig. 3. Note that the blood pressure in the experiment whose data are in Figs. 2 and 3 was lower than in the experiment of Fig. 6. In this model (18), as in experiments with rats (25), the amplitude of the TGF oscillation varies directly with arterial blood pressure. The greater amplitude of the frequency modulation in Fig. 6, compared with Fig. 3, could be attributed, at least in part, to the difference in blood pressures. System and measurement noise is another factor that could contribute to the difference in the modulation response. The data analyzed for Fig. 3 have all sources of noise for the measurement, whereas the data of Fig. 6 has only the variation in arterial blood pressure. Figure 7 compares the instantaneous frequency of the TGF oscillation with the frequency of the signal modulating myogenic amplitude and frequency. As can be seen in Fig. 7, both the TGF oscillation and the modulating signals occupy the same frequency band, a result consistent with the suggestion that the TGF signal is responsible for the modulation phenomena.

This set of simulations was designed to test whether known blood pressure fluctuations are a possible cause of the variation in amplitude and frequency modulation, and the results are consistent with the suggestion. The results do not exclude other sources of the variation.

DISCUSSION

We present the results of a model described in a companion paper (18) and designed to simulate single nephron blood flow,

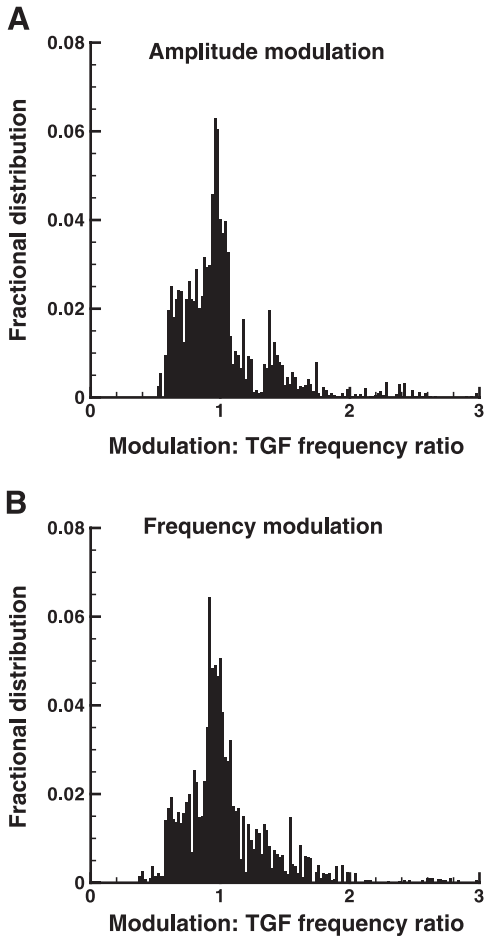

Fig. 5. The distribution of the ratio of frequencies from all experiments at normal blood pressure in (25). *A*: ratio of the frequency of amplitude modulation to the frequency of TGF. *B*: ratio of the frequency of frequency modulation to the frequency of TGF.

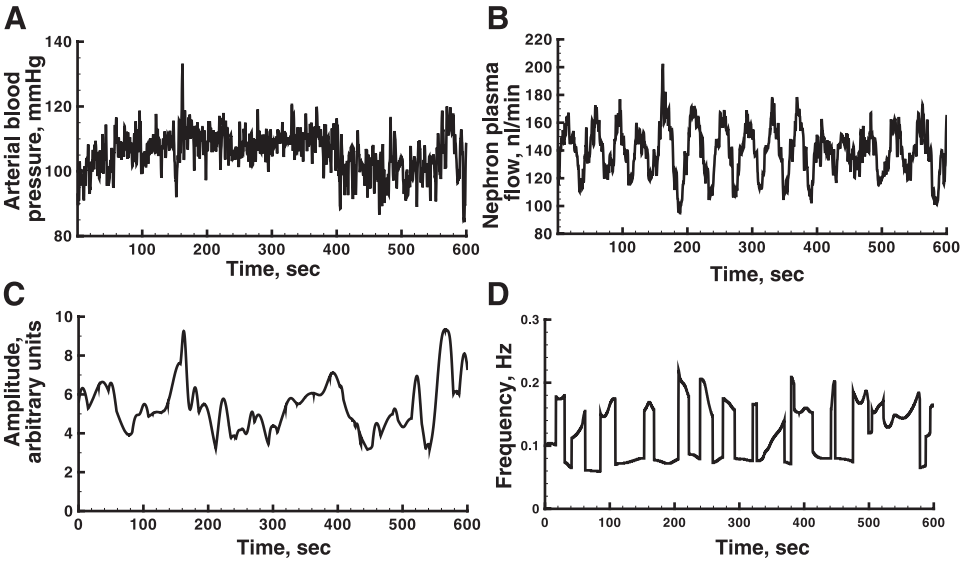

Fig. 6. Measured arterial blood pressure as input to the model. *A*: Mean arterial blood pressure. *B*: Nephron plasma flow rate predicted by the model using blood pressure in (*A*) as input. *C*: instantaneous amplitude of myogenic oscillation. *D*: instantaneous frequency of myogenic oscillation. Amplitude modulation units are the same as in Fig. 1.

GFR, tubular pressure, and NaCl concentration in tubular fluid at the macula densa, all of which have been measured (7, 9, 14–17, 25), and six intracellular variables in each of two afferent arteriolar segments, which have not been measured. As shown in the previous paper, the model predicts several features characteristic of the renal circulation in normotensive rats. These include steady state autoregulation of GFR and renal plasma flow over a blood pressure range of 80–135 mmHg; mean values of GFR, and filtration fraction consistent with experimental values; an oscillation due to the operation of TGF and reflected in all tubular variables; a smaller oscillation that operates at a higher frequency than TGF; and the same ratio of the frequencies of the two oscillations, as found experimentally. The mean proximal tubular pressure and the amplitude of a TGF-induced oscillation of tubular pressure are the same as measured experimentally, and the mean concentration of NaCl in tubular fluid and its TGF-induced oscillation are the same as found in experimental measurements. The oscillation of proximal tubular pressure leads the oscillation of early distal NaCl concentration. These results were obtained with a value of 100 mmHg for the mean arterial blood pressure, a value we consider to be normal for a halothane anesthetized rat, the standard source of the data being used for comparison. All these results are consistent with experimental observations. Moreover, the model reproduces these results over a range of values of ζ, the coupling coefficient, so that the result is not critically dependent on a particular value of this new coefficient.

In addition, the model predicted that TGF modulates the frequency and the amplitude of the myogenic oscillation. This result has not been reported previously. To detect this phenomenon, it is necessary to measure the frequency and the amplitude of the oscillation as continuous functions of time. The methods that permit this kind of analysis include time frequency analysis (2) and wavelet transforms (3). We selected wavelet transforms because the method permits the complete separation of amplitude and frequency information and provides quantitative information. With this technique one convolves a wavelet function with the time series to be analyzed. Appropriate selection of coefficients permits the analysis of specific frequencies. This procedure was applied to the simulation results and to measured single-nephron blood flow rate. The analysis of the simulation results shows that the amplitude varies in synchrony with the TGF oscillation. This result means that the amplitude of the myogenic oscillation varies. Close examination of the simulation's time series, Fig. 1*A*, shows the variation. The magnitude of the myogenic oscillation will depend on Ca_i. In the model, TGF is coupled to voltage-gated Ca channels. If fewer Ca channels open because of the action of TGF, Ca will not rise as much, and the myogenic oscillation will be attenuated, and vice versa.

Figure 1 also shows the frequency of the myogenic oscillation in the simulation result. The oscillation switches back and forth between frequencies of 0.096 and 0.141 Hz. The clock that triggers the myogenic oscillation comprises a set of voltage and Ca sensitive K channels, voltage-gated Ca channels, and a leak pathway. The three pathways interact and form an autonomous limit cycle, the myogenic oscillator (5, 18). A change in any of the ionic currents will change the clock rate. The TGF signal does not have a switch-like shape, but the system that generates the clock signal is nonlinear, and it is therefore to be expected that the frequency will not trace the TGF signal exactly.

We have previously used wavelet transforms with tubular pressure measurements (24), which have less noise than the blood flow; the results of that study and of the analysis of single-nephron blood flow in this one are in accord. Both the amplitude and the frequency modulation result with measured single-nephron blood flow show considerable variation with time, in contrast to the simulation result. The question at issue is to what extent variation in TGF is responsible for this variability. We developed the double-wavelet method to answer this question. The two time series of Fig. 3 were themselves subjected to wavelet transforms to determine the frequency of the modulation effect. Fig. 4 shows the result. The TGF frequency is also shown and is not constant. It does, however, remain within a fairly narrow frequency band. The frequencies of the amplitude and the frequency of the myogenic oscillation also vary within this same band. The similarity of the frequency bands is consistent with the hypothesis that

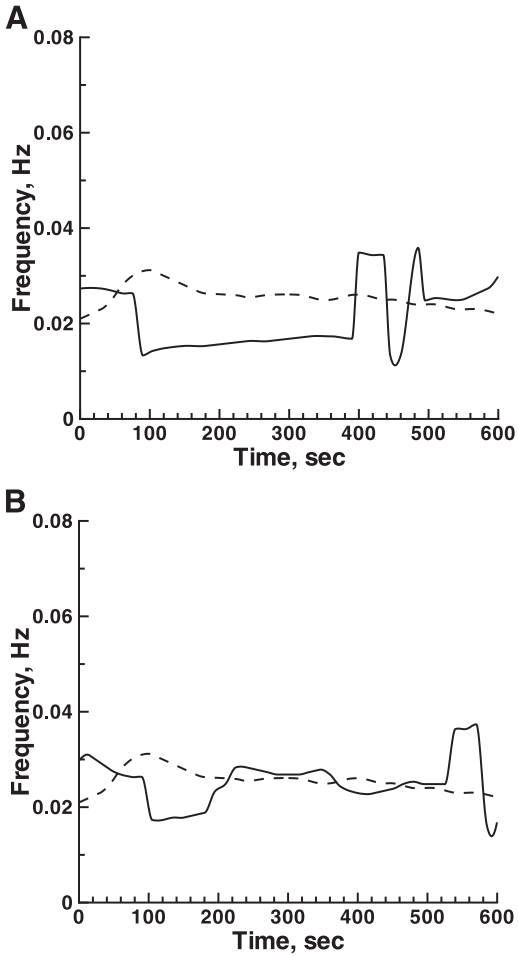

Fig. 7. Analysis of model results with measured arterial blood pressure, in Fig. 6. *A*: modulation frequency of amplitude modulation (solid line) and TGF frequency (dashed line), as functions of time. *B*: modulation frequency of frequency modulation (solid line) and TGF frequency (dashed line), as functions of time. The dashed lines are the same in the two panels.

the TGF signal modulates both the amplitude and the frequency of the myogenic oscillation, at least in this one experiment. Results from 10 rats were obtained in (25). We analyzed all 10 records and calculated the instantaneous ratio of the modulation frequency to the TGF frequency. This procedure generated ~50,000 data points. As can be seen in Fig. 5, the results cluster around a ratio of unity, which is also consistent with the hypothesis that TGF modulates the amplitude and the frequency of the myogenic oscillation.

We speculated that the naturally occurring fluctuations in mean arterial blood pressure could be responsible for at least part of the variability in TGF and therefore in the frequency and amplitude modulation. To test this suggestion, we used measured blood pressure records from conscious rats (10) as the input to the model. The arterial pressure in this record varied over nearly 60 mmHg. The model predicts that the amplitude of the TGF oscillation varies directly with the arterial pressure but that nephron plasma flow remains stable around a mean value of 140 nl/min. The amplitude of the myogenic oscillation varied at the frequency of TGF, but the largest changes occurred at times when the blood pressure changed values. Also, please note that the ordinate of the graph showing amplitude vs. time is larger than in Fig. 1. The results of Fig. 1 were obtained with a constant arterial pressure of 100 mmHg. The pressures in Fig. 6 were largely greater than 100 mmHg. The predicted amplitude of the myogenic oscillation varies with arterial pressure (see Fig. 10 in Ref. 18) and experimentally (25). The greater amplitude in Fig. 6 probably results from the higher pressures.

This numerical experiment also showed significant frequency modulation and considerable variability in that modulation. Recall that this is the same model that generated Fig. 1, with its regular switching of both amplitude and frequency. When a measured arterial pressure record is used as input to the model, both forms of modulation become more variable. We suggest therefore, that naturally occurring fluctuations in arterial pressure provide at least part of the cause of the variation in frequency and amplitude modulation.

We used voltage-gated Ca channels as the point in the cell that couples to TGF. We based this choice on the strict dependence of the myogenic mechanism on extracellular Ca, and the presence of voltage-gated Ca channels in the plasma membranes of the arteriolar cells. The behavior of the model matches experimental data on autoregulation and on system dynamics, as detailed above. There are other coupling points that have not been evaluated in this study but that may play an important role. There is experimental evidence to support the operation of these other mechanisms and no reason a priori to assume that the entire coupling burden is carried by a single mechanism. These include signals mediated through intracellular Ca stores; receptor-operated Ca channels, which also mediate actions on intracellular Ca stores (13, 19); and Ca-insensitive regulation, most likely an action on phosphorylation of myosin light chain (11). The phosphorylation mechanism is unlikely to produce significant frequency modulation because the action of this signaling pathway does not affect the constituents of the myogenic clock mechanism, but it could act in concert with other mechanisms. Store-operated Ca release is a very complex and important mechanism, but we are unable intuitively to predict its effect on system dynamics.

Nonlinear interactions between TGF and the myogenic mechanism are probably important signaling mechanisms in renal autoregulation. The two different forms of modulation we have presented, both of which arise from nonlinear interactions, solve two different problems. The first is time coordination and stabilization. The arterial pressure can change rapidly. Propagation of a pressure disturbance through the tubular system to the macula densa entails a delay of 10–15 s (18). The myogenic mechanism can respond to the same signal in a fraction of this time. Unless there is some way to coordinate the two mechanisms, they could act in an uncoordinated manner and fail to provide adequate autoregulation. Amplitude modulation should permit the actions of the two mechanisms to act cooperatively. In human-made control systems, the introduction of a fast, low-ampltidude signal inside the feedback loop of a nonlinear controller has the effect of narrowing the nonlinear sector and stabilizing the system (26, 27). Because TGF is a nonlinear system, its interaction with the myogenic mechanism improves the stability of autoregulation. When the blood pressure increases, the kidney needs the afferent arteriolar resistance to increase, and vice versa. Without some form of coordination between the two mechanisms, it is to be expected that the system would fail to respond as the kidney needs it to

and that the blood flow will fluctuate inappropriately. Amplitude modulation helps to prevent this.

Frequency modulation solves a second problem, which is the fidelity of signal transmission. Frequency modulation is well known in signal processing as a robust method for sending and receiving signals in a noisy environment. Arteriolar smooth muscle contraction is triggered by increasing Ca_i, but Ca has many more functions in these cells than controlling muscle contraction. It is no exaggeration to say that the Ca environment of these cells is noisy. Spatial inhomogeneity is one answer to this problem, and recent evidence points to localization of calmodulin with voltage-gated Ca channels, which are inhomogeneously distributed in the plasma membrane (21). Frequency modulation is another, complementary way to connect the signal and the target.

ACKNOWLEDGMENTS

Supported in part by National Institutes of Health grant DK15968 to D. J. Marsh, a grant from the EU Commission (BioSim, Project #005137) to N. H. Holstein-Rathlou, a grant from the Lundbeck Foundation to O.V. Sosnovtseva, and U.S. Civilian Research and Development Foundation for the Independent states of the Former Soviet Union grants SR-006-X1 and Y1-P-06–06 to A.N. Pavlov.

REFERENCES

1. **Casellas D and Moore LC.** Autoregulation and tubuloglomerular feedback in juxtamedullary glomerular arterioles. *Am J Physiol Renal Fluid Electrolyte Physiol* 258: F660–F669, 1990.
2. **Chon KH, Raghavan R, Chen YM, Marsh DJ, and Yip KP.** Interactions of TGF-dependent and TGF-independent oscillations in tubular pressure. *Am J Physiol Renal Physiol* 288: F298–F307, 2005.
3. **Daubechies I.** The wavelet transform. Time-frequency localization and signal analysis. *IEEE Trans Inform Theory* 36: 961–1005, 1990.
4. **Deen WM, Robinson CR, and Brenner BM.** A model of glomerular ultrafiltration in the rat. *Am J Physiol* 223: 1178–1183, 1972.
5. **Gonzalez-Fernandez JM and Ermentrout GB.** On the origin and dynamics of the vasomotion of small arteries. *Math Biosci* 240: 127–167, 1994.
6. **Holstein-Rathlou NH and Marsh DJ.** A dynamic model of renal blood flow autoregulation. *Bull Math Biol* 56: 411–430, 1994.
7. **Holstein-Rathlou NH and Marsh DJ.** Oscillations of tubular pressure, flow, and distal chloride concentration in rats. *Am J Physiol Renal Fluid Electrolyte Physiol* 256: F1007–F1014, 1989.
8. **Holstein-Rathlou NH and Marsh DJ.** A dynamic model of the tubuloglomerular feedback mechanism. *Am J Physiol Renal Fluid Electrolyte Physiol* 258: F1448–F1459, 1990.
9. **Holstein-Rathlou NH and Leyssac PP.** TGF-mediated oscillations in the proximal intratubular pressure: differences between spontaneously hypertensive rats and Wistar-Kyoto rats. *Acta Physiol Scand* 126: 333–339, 1986.
10. **Holstein-Rathlou NH, He J, Wagner AJ, and Marsh DJ.** Patterns of blood pressure variability in normotensive and hypertensive rats. *Am J Physiol Regul Integr Comp Physiol* 269: R1230–R1239, 1995.
11. **Horowitz A, Menice CB, Laporte R, and Morgan KG.** Mechanisms of smooth muscle contraction. *Physiol Rev* 76: 967–1003, 1996.
12. **Layton HE, Pitman EB, and Moore LC.** Nonlinear filter properties of the thick ascending limb. *Am J Physiol Renal Physiol* 273: F625–F634, 1997.
13. **Lee CH, Poburko D, Kuo KH, Seow CY, and Van Breeman C.** Ca oscillations, gradients, and homeostasis in vascular smooth muscle. *Am J Physiol Heart Circ Physiol* 282: H1571–H1583, 2002.
14. **Leyssac PP.** Further studies on oscillating tubuloglomerular feedback responses in the rat kidney. *Acta Physiol Scand* 126: 271–277, 1986.
15. **Leyssac PP and Baumbach L.** An oscillating intratubular pressure response to alterations in Henle loop flow in the rat kidney. *Acta Physiol Scand* 117: 415–419, 1983.
16. **Leyssac PP and Holstein-Rathlou NH.** Effects of various transport inhibitors on oscillating tubuloglomerular feedback pressure responses in the rat. *Pflügers Arch* 407: 285–291, 1986.
17. **Leyssac PP and Holstein-Rathlou NH.** Tubuloglomerular feedback: enhancement in spontaneously hypertensive rats and effects of anesthetics. *Pflügers Arch* 413: 267–272, 1989.
18. **Marsh DJ, Sosnovtseva OV, Chon K, and Holstein-Rathlou NH.** Nonlinear interactions in renal blood flow regulation. *Am J Physiol Regul Integr Comp Physiol* 288: In press.
19. **McFadzean I and Gibson A.** The developing relationship between receptor-operated and store-operated calcium channels in smooth muscle. *Br J Pharmacol* 135: 1–13, 2002.
20. **Moore LC, Rich A, and Casellas D.** Ascending myogenic autoregulation: interactions between tubuloglomerular feedback and myogenic mechanisms. *Bull Math Biol* 56: 391–410, 1992.
21. **Mori MX, Erickson MG, and Yue DT.** Functional stoichiometry and local enrichment of calmodulin interacting with Ca_i^{2+} channels. *Science* 304: 432–435, 2004.
22. **Sakai T, Craig DA, Wexler AS, and Marsh DJ.** Fluid waves in renal tubules. *Biophys J* 50: 805–813, 1986.
23. **Smedley GT, Yip KP, Wagner AJ, Dubovitsky S, and Marsh DJ.** A laser Doppler velocimetry instrument for in-vivo measurements of blood flow in single renal arterioles. *IEEE Trans Biomed Eng* 40: 290–297, 1993.
24. **Sosnovtseva OV, Pavlov AN, Mosekilde E, Holstein-Rathlou NH, and Marsh DJ.** A double-wavelet approach to study frequency and amplitude modulation in renal autoregulation. *Phys Rev E Stat Nonlin Soft Matter Phys Epub* 031915 70: 1–8, 2004.
25. **Yip KP, Holstein-Rathlou NH, and Marsh DJ.** Mechanisms of temporal variation in single-nephron blood flow in rats. *Am J Physiol Renal Fluid Electrolyte Physiol* 264: F427–F434, 1993.
26. **Zames G and Schneyder NA.** Dither in nonlinear systems. *IEEE Trans Automatic Control* 21: 660–667, 1976.
27. **Zames G and Schneyder NA.** Structural stabilization and quenching by dither in nonlinear systems. *IEEE Trans Automatic Control* 22: 352–361, 1977.